

# Analysis of the wind loading of square cylinders using covariance proper transformation

Enrico T. de Grenet<sup>†</sup>

*Department of Civil Engineering, University of Florence, Via S. Marta, 3 50139, Florence, Italy*

Francesco Ricciardelli<sup>‡</sup>

*Department of Mechanics and Materials, University of Reggio Calabria,  
Via Graziella, Feo di Vito 89060, Reggio Calabria, Italy*

*(Received March 7, 2003, Accepted November 28, 2003)*

**Abstract.** In this paper the capacity of Covariance Proper Transformation (CPT) analyses to provide information about the wind loading mechanisms of bluff bodies is investigated through the application to square cylinders. CPT is applied to the fluctuating pressure distributions on a single cylinder, as well as on a pair of cylinders in the tandem and side by side arrangements, with different separations. Both smooth and turbulent flow conditions are considered. First, through the analysis of the contributions of each CPT mode to the total fluctuating aerodynamic forces, a correspondence between modes and aerodynamic components is sought, which is then verified through examination of the mode shapes. When a correspondence between modes and aerodynamic components is found, an attempt is made to separate the different frequency contributions to the aerodynamic forces, provided by each mode. From the analyses it emerges that (a) in most cases each mode is associated to one single force component, that (b) retaining a limited number of modes allows reproducing the aerodynamic forces with a rather good accuracy, and that (c) each mode is mainly associated with one frequency of excitation.

**Keywords:** wind loading; pressure fluctuations; Covariance Proper Transformation; wind tunnel testing; square cylinders.

---

## 1. Analysis of the wind loading using Covariance Proper Transformation

In the last decade applications of Covariance Proper Transformation to the analysis of the fluctuating wind forces appeared in the literature. Besides the computational advantage that CPT may or may not bring to the evaluation of the structural response, when only a limited number of modes is retained, CPT can be used as a tool to investigate the mechanisms of the dynamic wind loading of structures. Different types of structures have been considered by different authors, and there seem not to be a general agreement on whether CPT allows one to single out the different excitation mechanisms, and to provide insight of their physics. For a low-rise building, Holmes, *et al.* (1997) did not find any correspondence between the covariance modes and the physical

---

<sup>†</sup> Ph.D. Candidate

<sup>‡</sup> Associate Professor

phenomena contributing to the wind excitation, which instead was found by Tamura, *et al.* (1997). On the other hand, for a tall building, Kikuchi, *et al.* (1997), and Tamura, *et al.* (1999) found a correspondence between covariance modes and aerodynamic components. Baker (2000 and 2001) also found some correspondence between the first modes and the causes of excitation, for a cube, a wall and a low-rise building. Ricciardelli, *et al.* (2002) applied CPT to the analysis of the wind loading on a fixed and vibrating bridge box deck in smooth flow, and found that there is evidence of a correspondence between the first covariance modes and the different mechanisms of excitation existing at the different vibration regimes.

In this paper, CPT is applied to the fluctuating pressure distributions on a square cylinder and on a pair of square cylinders placed in tandem and side by side arrangements, in both smooth and turbulent flow. Discussion of the wind loading on a pair of square cylinders have already been published, which did not include CPT analyses (Ricciardelli 1994, Ricciardelli and Vickery 1994 and 1998). This paper, more than an attempt to a further insight on the aerodynamics of square cylinders, presents an investigation on the limits of CPT analysis as a tool for the understanding of the mechanism of wind loading of bluff bodies. A CPT analysis of the pressure fluctuations on square section have already been presented in Lee (1975), where the amount of energy associated with the first mode is analysed for different flow conditions.

### 1.1. Covariance Proper Transformation of pressure fields

Proper Orthogonal Decomposition (POD) is the expansion of a multivariate, correlated random process into the combination of a number of monovariate, uncorrelated processes, through the use of orthogonal modes (Solari and Carassale 2000). POD can be applied in the time domain, in which case it is called Covariance Proper Transformation (CPT), or in the frequency domain, in which case it is termed Spectral Proper Transformation (SPT).

With specific reference to pressure fluctuations, covariance modes are obtained from the non-trivial solution of the homogenous equation:

$$(\mathbf{C}_{C_p} - \lambda_i \mathbf{I}) \phi_i = 0 \quad (1)$$

in which  $\mathbf{C}_{C_p}$  is the covariance matrix of the correlated  $N$ -variate process:

$$\mathbf{C}_p(t) = \frac{1}{1/2\rho U^2} [p_1(t) \dots p_i(t) \dots P_N(t)]^T \quad (2)$$

whose components are the instantaneous pressure coefficients at points on the body surface. In Eq. (1)  $\mathbf{I}$  is the identity matrix, and  $\lambda_i$  and  $\phi_i$  are the  $i$ -th eigenvalue and eigenvector, respectively. The covariance matrix can then be written as:

$$\mathbf{C}_{C_p} = \mathbf{\Phi} \mathbf{\Lambda} \mathbf{\Phi}^T = \sum_i \phi_i \phi_i^T \lambda_i \quad (3)$$

where  $\mathbf{\Lambda}$  is the diagonal matrix listing the eigenvalues  $\lambda_i$ , and  $\mathbf{\Phi}$  is the matrix whose columns are the eigenvectors  $\phi_i$ . The time history of the multivariate correlated process  $\mathbf{C}_p(t)$  can be expressed

as a linear combination of monovariate, uncorrelated processes  $x_i(t)$ :

$$\mathbf{C}_p(t) = \mathbf{\Phi}\mathbf{x}(t) = \sum_{i=1}^N \phi_i x_i(t) \quad (4)$$

where  $\mathbf{x}(t)$  is the image of the process  $\mathbf{C}_p(t)$  in the eigenvectors space, and its covariance matrix coincides with the diagonal matrix of the eigenvalues  $\mathbf{\Lambda}$ .

The CPT analyses that will be presented in this paper are based on wind tunnel pressure measurements on cylinders provided with 8 pressure taps on each side, therefore  $N=32$  when a single cylinder is considered, and  $N=64$  when the pair of cylinders is considered.

### 1.2. Methodology of analysis

In Ricciardelli, *et al.* (2002) it was shown how CPT can identify the different mechanisms of aeroelastic excitation of a vibrating bridge box deck. In particular, it was observed that (a) a limited number of modes is sufficient to reproduce the lift and torque components, (b) there exists a correspondence between covariance modes and the different mechanism of excitation, and (c) it is usually possible to identify pairs of modes reproducing the in-phase and the out-of-phase components of each aerodynamic action. In this paper, an attempt is made to corroborate the belief that CPT allows one to single out the different mechanism of the aerodynamic excitation.

In Ricciardelli, *et al.* (2002) the analyses were organised in a four-level pattern. At the first level, a correspondence between modes and components of the aerodynamic action (lift and torque) was sought. When this correspondence was found, the mode shapes were analysed to recognize the different space distribution of the pressure fluctuations that contribute to the same aerodynamic component (second level, space domain). At the third level of analysis, the mechanisms of excitation associated with each mode were recognised, from comparison of the spectra of the aerodynamic forces with the spectra of the image processes  $x_i(t)$  (frequency domain). In many cases it was found that pair of modes exist, associated with the same aerodynamic component and acting at the same frequency. When such pairs were found, the phase lag between the image processes associated with the two modes was sought (fourth level, time domain), which in many cases turned out to be  $\pi/2$ . The two modes were, therefore, postulated to correspond to the in-phase and out-of-phase components of the same mechanism of excitation.

## 2. Experimental setup

The data used in the analyses are the results of tests carried out at the Boundary Layer Wind Tunnel Laboratory (BLWTL) of the University of Western Ontario. The model was made of two aluminium square cylinders 1.20 m long, with a cross-section of a 3 cm side. Each cylinder had its midspan section instrumented with eight pressure taps on each side (Fig. 1). The two cylinders were placed horizontally in the wind tunnel, in a way to obtain two-dimensional flow conditions at the section of measurement. The mount was such that the distance between the cylinders could be varied, as well as the angle of attack. Values of the ratio of the centre-to-centre distance  $s$  to the side of the square  $b$ , in the range of 2 to 13 were considered, together with angles of attack in the range of  $0^\circ$  to  $90^\circ$ . Tests were carried in smooth and turbulent flow conditions, with wind speeds of

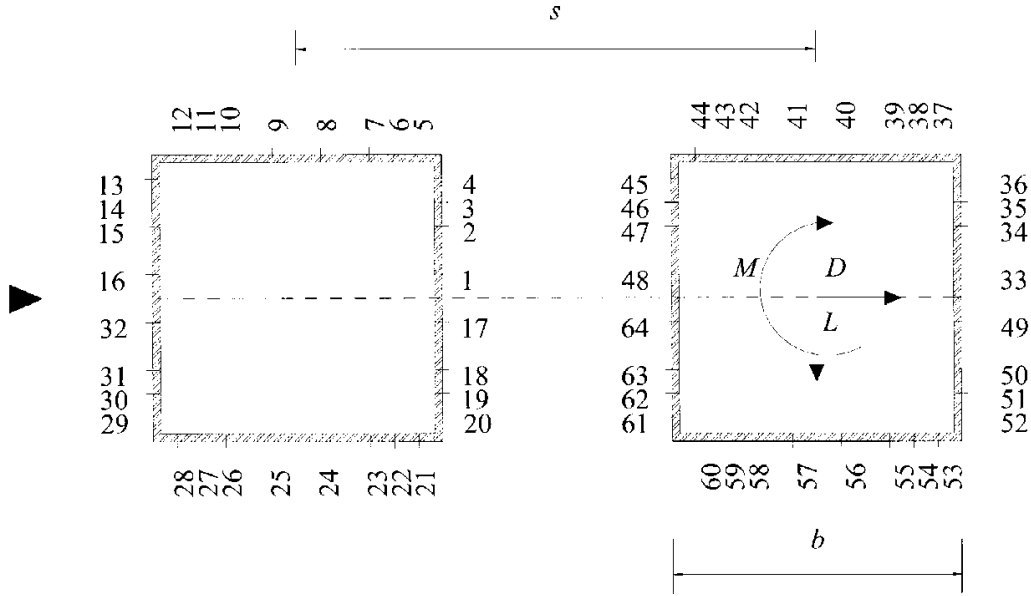


Fig. 1 Pressure tap distribution and numbering on the cross section of the two cylinders

10.7 m/s and 6.6 m/s, respectively. The turbulent flow, generated with the use of a coarse grid, had an intensity of turbulence of 0.10 and an integral scale of 0.24 m. Measurements were taken for 256s at a sampling rate of 200 Hz. All the details concerning the experimental setup can be found in Ricciardelli (1994).

In this paper, the results of CPT analyses of the pressure fluctuations on the single cylinder in smooth and turbulent flow are presented. In addition, the pair of cylinders at angles of attack of  $0^\circ$  (tandem arrangement) and  $90^\circ$  (side by side arrangement) will be considered, for separations  $s/b=2$ , 4 and 13. The analyses for the single cylinder was based on the measurements on the upstream cylinder in the tandem arrangement at  $s/b=13$ , which guarantees that there is no interaction with the downstream cylinder.

### 3. Results for the single cylinder

To evaluate the amount of energy associated with each covariance mode, the parameter:

$$\Lambda_n = \frac{\sum_{i=1}^n \lambda_i}{\sum_{i=1}^{32} \lambda_i} \quad (5)$$

was used, i.e., the ratio of the sum of the first  $n$  eigenvalues to the sum of the  $N=32$  eigenvalues, which is a measure of the contribution of the first  $n$  modes to the total aerodynamic excitation.

In Fig. 2, the  $\Lambda_n$  coefficients are plotted for the two flow conditions. It appears how the contribution of the first mode to the total excitation ranges between 49% and 86%, while the contribution of the first eight modes is in the range of 98% to 99%. The figure also shows that in

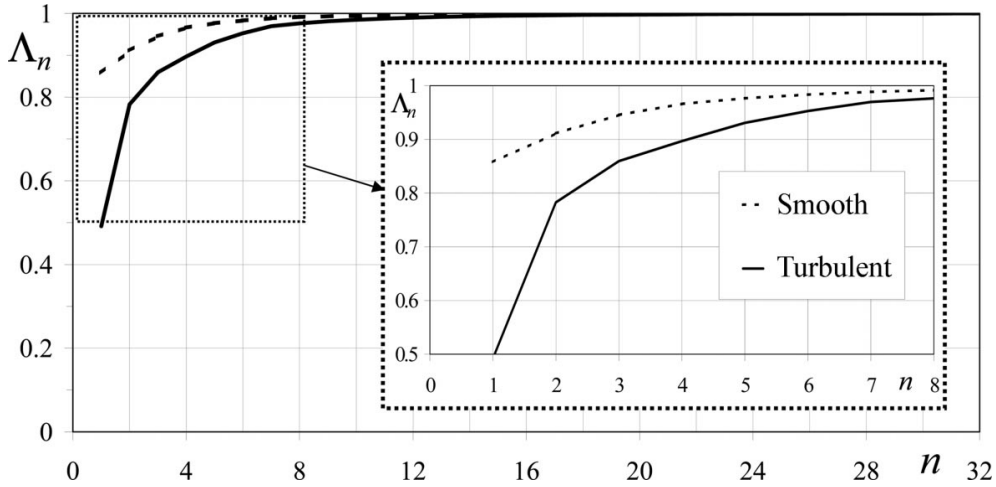


Fig. 2  $\Lambda_n$  coefficients for the single cylinder in smooth and turbulent flow

smooth flow a lower number of modes is sufficient to reach the same amount of energy than in turbulent flow. In the following it will be shown that modes can be associated with mechanisms of excitation, and in smooth flow a lower number of mechanisms of excitation co-exist, which explains the lower number of modes required to reach the same amount of energy of the pressure fluctuations.

As a second step, to measure the contribution of the covariance modes to each aerodynamic component, the partial (instantaneous) aerodynamic coefficients associated with the  $i$ -th mode were defined as:

$$C_{Di}(t) = \frac{1}{b} \gamma_D^T \alpha \phi_i x_i(t) = \gamma_D^T \mathbf{P}_i(t) \quad (6)$$

$$C_{Li}(t) = \frac{1}{b} \gamma_L^T \alpha \phi_i x_i(t) = \gamma_L^T \mathbf{P}_i(t)$$

where  $\gamma_D$  and  $\gamma_L$  are 32-component vectors containing the cosines of the angles between the (inward) normal to the cylinder surface at each pressure tap location, and the (positive) alongwind and acrosswind directions, respectively, and where  $\alpha$  is the  $32 \times 32$  diagonal matrix whose elements are the tap tributary areas.

In Fig. 3, the ratios of the variance of the partial aerodynamic coefficients associated with the first eight modes, to the variance of the (total) aerodynamic coefficients are shown:

$$\Delta_{Di} = \tilde{C}_{Di}^2 / \tilde{C}_D^2 \quad (7)$$

$$\Delta_{Li} = \tilde{C}_{Li}^2 / \tilde{C}_L^2$$

It can be observed that, both in smooth and turbulent flow, each mode is associated with one

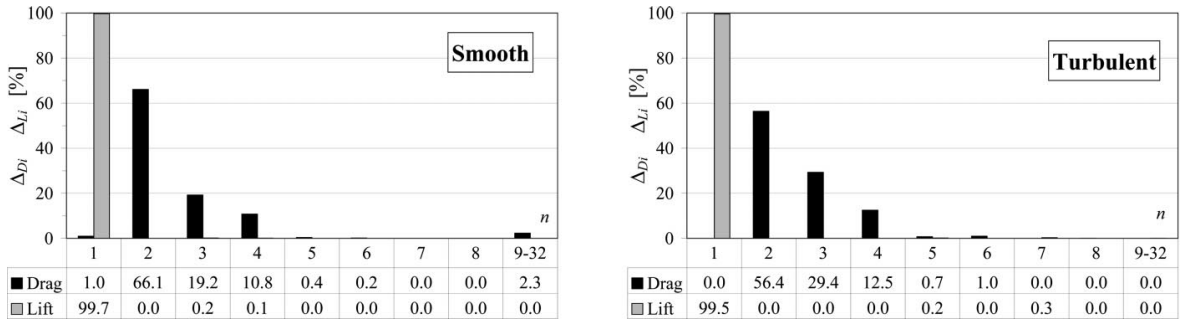


Fig. 3  $\Delta_{D_j}$  and  $\Delta_{L_j}$  coefficients for the single cylinder in smooth and turbulent flow

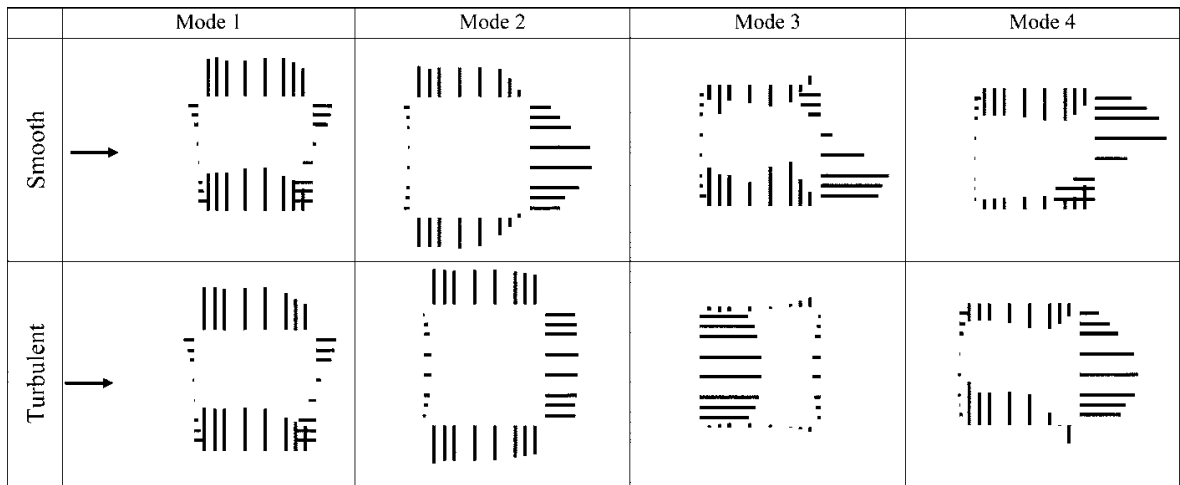


Fig. 4 First four mode shapes for the single cylinder in smooth and turbulent flow

single aerodynamic component. The first mode is always an acrosswind mode, and contributes to the lift with 99.7% in smooth flow and with 99.5% in turbulent flow. The remaining modes are mainly alongwind modes and, if only the first eight modes are retained less than 2.3% of drag is neglected.

In Fig. 4 the first four covariance mode shapes are plotted for the two flow conditions. In agreement with what observed about Fig. 3, it is possible to see that the first mode shape is clearly associated with lift, while mode shapes two, three and four are associated with drag. In particular, in both smooth and turbulent flows mode two corresponds to a symmetric fluctuating pressure distribution on the leeward face of the cylinder, and is, therefore, related to wake turbulence. In smooth flow, modes three and four are again associated with pressure fluctuations on the leeward face, but the distribution is almost antisymmetric. In turbulent flow, mode three is associated with pressure fluctuations on the windward face, and therefore related to the oncoming turbulence, while mode four is again a symmetric mode related to wake turbulence.

Once a correspondence between modes and aerodynamic components is found, comparison of the spectra of the partial aerodynamic coefficients defined through Eqs. (6), with those of the total

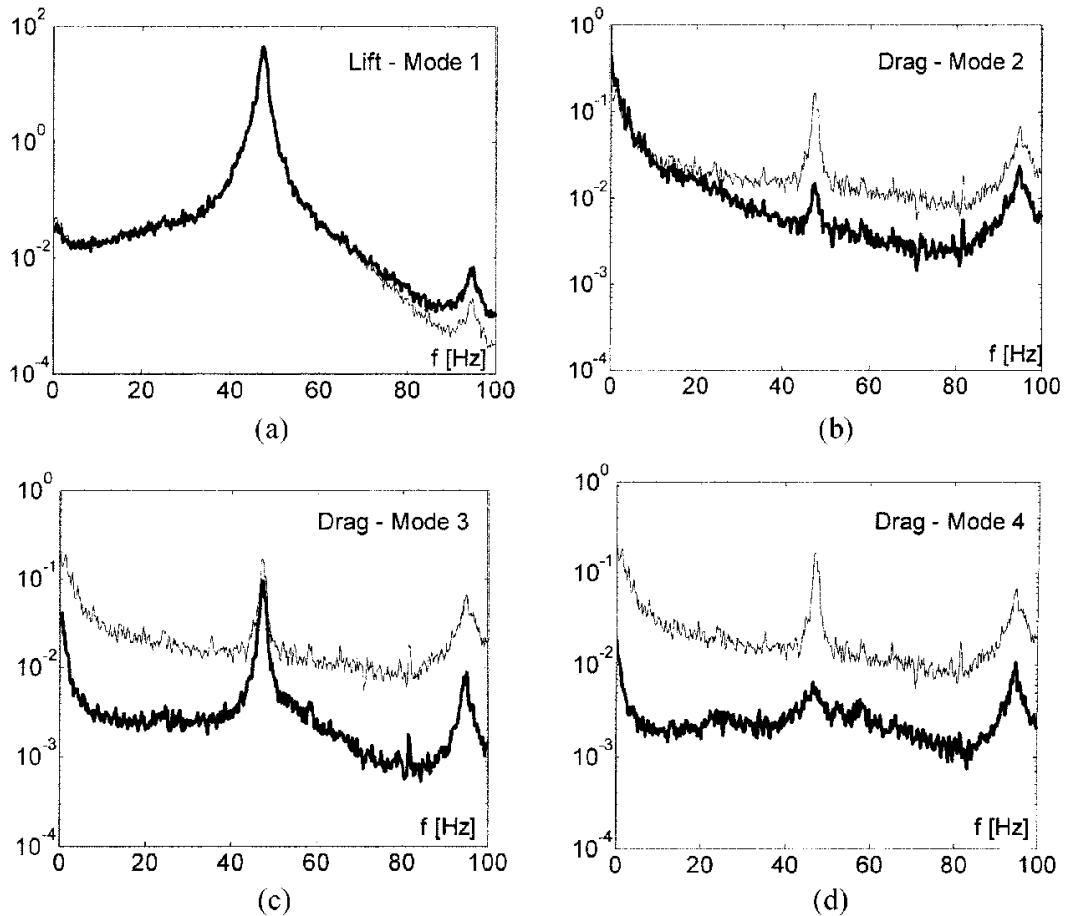


Fig. 5 Spectra of the partial (thick line) and total (thin line) aerodynamic coefficients for the single cylinder in smooth flow

aerodynamic coefficients allows seeking a relation between covariance modes and the different physical causes of excitation. As an example, in Fig. 5(a) the spectrum of the partial lift coefficient  $C_{L1}$  in smooth flow is shown, confirming that the first mode alone is sufficient to reproduce the lift component in a broad range of frequencies. In Figs. 5(b)-(d), the spectra of the partial drag coefficients  $C_{D2}$ ,  $C_{D3}$ ,  $C_{D4}$  in smooth flow are shown. Figs. 4 and 5 suggest that modes two and four provide the symmetric and antisymmetric components at twice the Strouhal frequency, while mode three provides the antisymmetric component at the Strouhal frequency. Altogether modes two, three and four provide 96.1% of the total drag excitation.

#### 4. Results for the pair of cylinders in tandem arrangement

For a pair of square cylinders placed in tandem arrangement, Ricciardelli and Vickery (1998) showed that three types of aerodynamic interaction can take place. For very small separations, ( $s/b < 3$ )

the flow separates from the upstream cylinder and reattaches to the downstream cylinder, making the aerodynamics very similar to that of a single, elongated rectangle. For intermediate separations ( $3 < s/b < 5$ ) the two cylinders behave as separated bodies, but a two way interaction takes place, that is, the pressure distribution on both cylinders is different from that of the isolated cylinder. For larger separations ( $s/b > 5$ ) a one way interference takes place, being only the pressure distribution on the downstream cylinder affected by the upstream cylinder. In addition, it was found that for intermediate to large separations, the interaction is of a convective nature. This means that the average time lag between peak values of the shedding-induced forces on the two cylinders is linearly related to the separation, and convective velocities of vortices of 80% and 78% of the oncoming wind speed were estimated in smooth and turbulent flow, respectively. This brings that the phase between the acrosswind forces acting on the two cylinders has also a linear variation with separation, being zero for  $s/b=4$  and for  $s/b=10$ , and being equal to  $\pi$  for  $s/b=7$ . As a consequence, the shedding induced acrosswind forces on each of the two cylinders mostly contribute to the overall lift on the pair of cylinders for  $s/b=4$  and for  $s/b=10$ , but result in torque for  $s/b=7$ . For separations other than these, when the phase between vortex shedding from the two cylinders is neither zero nor  $\pi$ , then the shedding induced acrosswind forces on the two cylinders contribute to both lift and torque of the pair.

This result was confirmed by the CPT analyses, as it was found that for separations at which shedding induced forces on the two cylinders are in phase or out of phase, the first covariance mode is associated with one single aerodynamic component (lift or torque, respectively), whereas when the phase is neither zero nor  $\pi$ , coupling exists between lift and torque modes of the pair.

For the pair of cylinders most of the aerodynamic torque is the result of out-of-phase lift forces applied to the two cylinders, therefore the torque coefficient is defined as:

$$C_M = \frac{M}{1/2\rho U^2 b s} = \frac{b}{s}(C_{Mu} + C_{Md}) + \frac{1}{2}(C_{Lu} - C_{Ld}) \quad (8)$$

where  $C_{Lu}$ ,  $C_{Ld}$ ,  $C_{Mu}$  and  $C_{Md}$  are the lift and torque coefficients of the upstream and downstream cylinders, respectively.

For the pair, the partial drag and lift coefficients take the same expressions as those given for the single cylinder in Eqs. (6), where the size of vectors and matrices is changed to 64. Using the same notation of Eq. (6), the partial torque coefficient is defined for the pair of cylinders:

$$C_{Mi}(t) = \frac{1}{b s} \gamma_M^T \alpha \phi_i x_i(t) = \frac{1}{s} \gamma_M^T \mathbf{P}_i(t) \quad (9)$$

where  $\gamma_M$  is the 64-component vector containing the distances of the (inward) normal to the cylinder surface at the pressure tap locations, to the common centre of the pair, with plus or minus sign, depending on whether the normal rotates clockwise or counter clockwise with respect to the common centre.

#### 4.1. Spacing to breadth ratio equal to four

In Fig. 6 the ratios  $\Delta_{Di}$  and  $\Delta_{Li}$  defined through Eq. (7), and the corresponding coefficient:

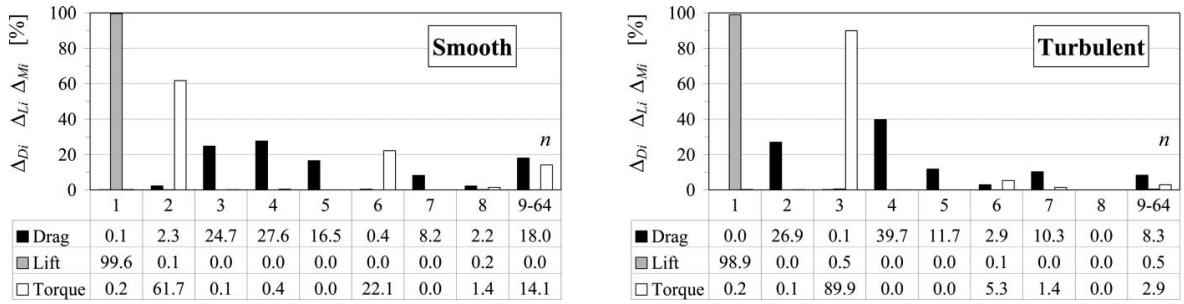


Fig. 6  $\Delta_{D_j}$ ,  $\Delta_{L_j}$  and  $\Delta_{M_j}$  coefficients for the pair of cylinders in tandem arrangement for  $s/b=4$  in smooth and in turbulent flow

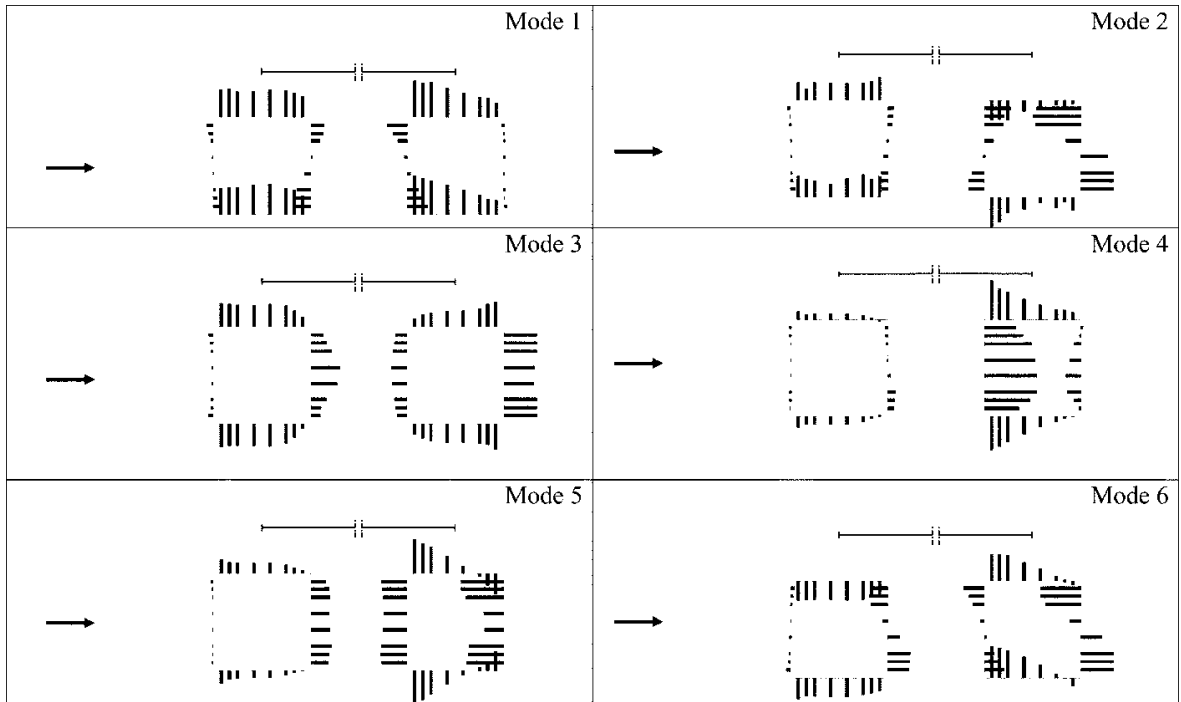


Fig. 7 First six mode shapes for the pair of cylinders in tandem arrangement for  $s/b=4$  in smooth flow

$$\Delta_{M_i} = \tilde{C}_{M_i}^2 / \tilde{C}_M^2 \quad (10)$$

associated with torque, are shown for  $s/b=4$ . The figure shows that also for the pair of cylinders in tandem arrangement with  $s/b=4$ , and both in smooth and turbulent flow conditions, CPT decouples the aerodynamic forces, and that the first mode is in always a lift mode.

The first six mode shapes for the pair of cylinders in tandem arrangement at  $s/b=4$  are shown in Fig. 7, for the smooth flow condition, which confirms the results shown in Fig. 6. Mode one is a lift mode, deriving from in-phase lift forces on the two cylinders, while mode two is a torque mode, deriving from out-of-phase lift forces on the two cylinders. Modes three to five are all almost

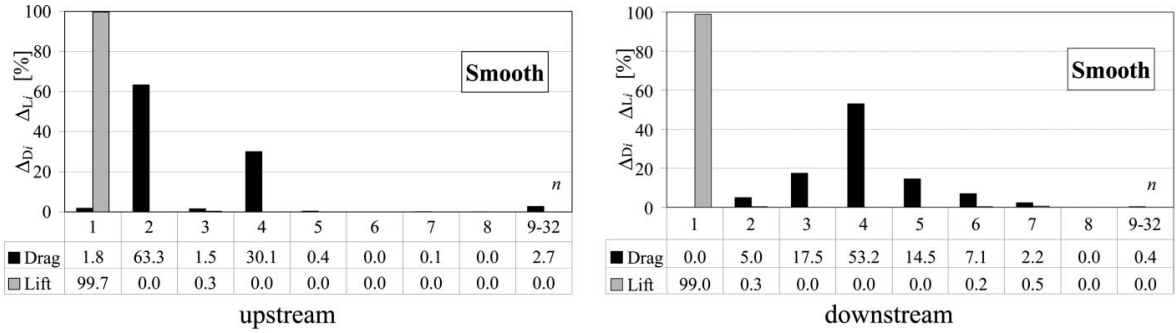


Fig. 8  $\Delta_{D_i}$  and  $\Delta_{L_i}$  coefficients evaluated on the upstream and downstream cylinders in tandem arrangement for  $s/b=4$  in smooth flow

symmetric drag modes. Modes three and five seem to be both associated with wake turbulence, as pressure fluctuations on the windward face of the upstream cylinder are almost zero, while pressure fluctuations take place on the leeward face of the upstream cylinder and on the windward and leeward faces of the downstream cylinder. Mode four, on the other hand, seems to be associated with the pressure fluctuations induced on the downstream cylinder by the vortices shed from the upstream cylinder. Mode six is again a torque mode, mainly deriving from out-of-phase lift forces on the two cylinders, but with larger contributions, with respect to mode two, of the torque acting on each on the two cylinders, i.e. of the first term in the right hand side of Eq. (8).

To investigate the nature of the aerodynamic interaction, the ratios  $\Delta_{D_i}$  and  $\Delta_{L_i}$  defined through Eq. (7) are shown in Fig. 8, as evaluated on the two cylinders separately, in smooth flow. From comparison of Figs. 3 and 8, the two way interaction between the cylinders is clear, as the distribution of the  $\Delta_{D_i}$  and  $\Delta_{L_i}$  coefficients for both the upstream and downstream cylinders (Fig. 8) is different from that of the single cylinder (Fig. 3). In Fig. 9 modes one and two of the upstream cylinder and modes one and three of the downstream cylinder are shown, as evaluated on the two cylinders separately. Although modes one and two of the upstream cylinder have the same shape as modes one and two of the single cylinder (compare Figs. 4 and 9), and provide the same contribution to the total lift and drag actions (compare Figs. 3 and 8), the higher modes of the upstream cylinder not only have different shapes from those of the single cylinder, but also provide different contributions to the total aerodynamic forces. On the other hand, there is no correspondence between the modes of the downstream cylinder and those of the single cylinder. Although mode one is in both cases a lift mode, the corresponding shapes are different. In addition, mode three of the downstream cylinder is a drag mode associated with pressure fluctuations on the windward face, therefore related to the turbulence generated by the upstream cylinder, and such a mode does not exist for the single cylinder.

It is also of interest to compare the mode shapes of each cylinder of the pair, to those of the pair of cylinders (Figs. 9 and 7, respectively). It can be observed that, if combined, modes one of the two cylinders reproduce mode one of the pair, while mode two of the upstream cylinder and mode three of the downstream cylinder can be recognised in modes three and four of the pair.

A similar comparison was carried out for the turbulent flow condition, and in Fig. 10 the first four mode shapes for the pair of cylinders are shown. Modes one and three are lift and torque modes associated with in-phase and out-of-phase lift forces on the two cylinders, respectively. Modes two

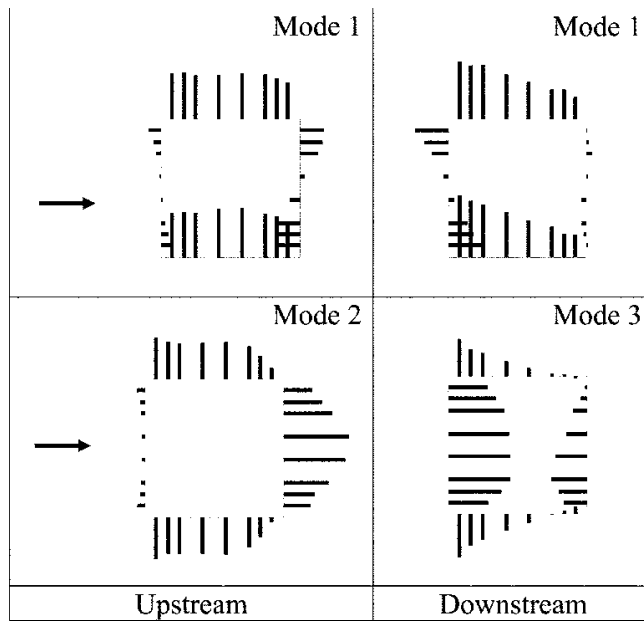


Fig. 9 First and second mode shape for the upstream cylinder and first and third mode shape for the downstream cylinder in tandem arrangement for  $s/b=4$  in smooth flow

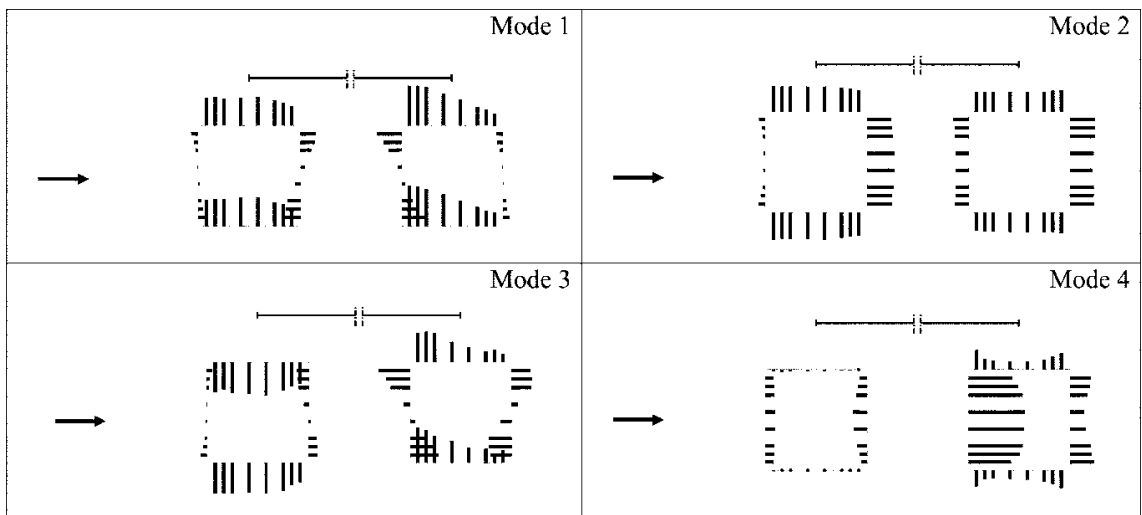


Fig. 10 First four mode shapes for the pair of cylinders in tandem arrangement for  $s/b=4$  in turbulent flow

and four are symmetric drag modes, and, as observed for the smooth flow condition, they seem to be associated with wake turbulence and with vortex shedding from the upstream cylinder, respectively.

4.2. Spacing to breadth ratio equal to two

As earlier mentioned, for very small separations the flow reattaches on the downstream cylinder, making the pair behave as one single, elongated rectangle. In this condition, CPT is not always successful in decoupling the aerodynamic components. In Fig. 11 the ratios  $\Delta_{D_i}$ ,  $\Delta_{L_i}$  and  $\Delta_{M_i}$  are plotted for the pair of cylinders at  $s/b=2$ , both in smooth and turbulent flow, showing how in smooth flow modes one and two contribute to more than one aerodynamic component. In Fig. 12 the first two mode shapes are shown, indicating that mode one is associated with pressure fluctuations only on the downstream cylinder, and in particular with large, and opposite sign fluctuations on the side faces, small, antisymmetric fluctuations on the windward face, and almost no fluctuations on the leeward face. This is clearly a mode associated with flow reattachment on the downstream cylinder, and provides contributions to lift (96.8%) and torque (74.1%), together with a minor contribution to drag (7.0%). For mode two, a lift force derives from the upstream cylinder, combined with a complex pressure distribution on the downstream cylinder. The lift forces on the two cylinders, however, cancel out, and the resulting action is a drag force (55.7% of the total drag) resulting from a non-symmetric pressure distribution, therefore combined with torque (14.8% of the total torque). In Fig. 13 the spectra of the partial lift and torque coefficient associated with mode one (a and b), and of the partial drag and torque coefficients associated with mode two (c and d), are shown. Fig. 13(a)-(b) shows that mode one reproduces lift in the whole frequency range, and torque around the Strouhal frequency and for frequencies larger than that. Mode two (Fig. 13(c)-(d))

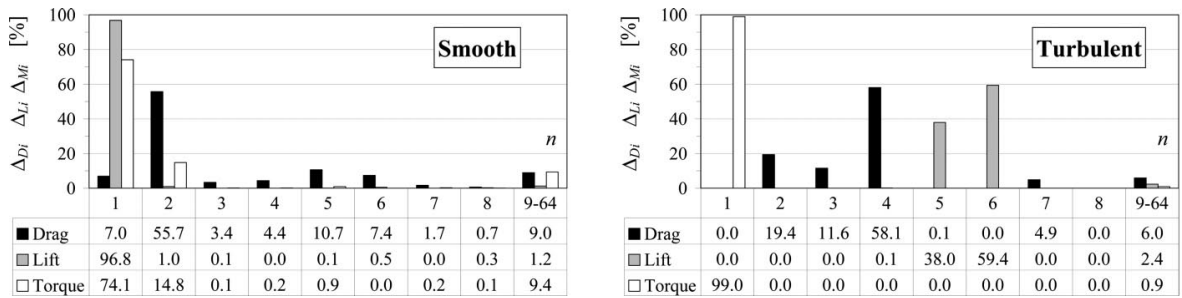


Fig. 11  $\Delta_{D_j}$ ,  $\Delta_{L_j}$  and  $\Delta_{M_j}$  coefficients for the pair of cylinders in tandem arrangement for  $s/b=2$  in smooth and in turbulent flow

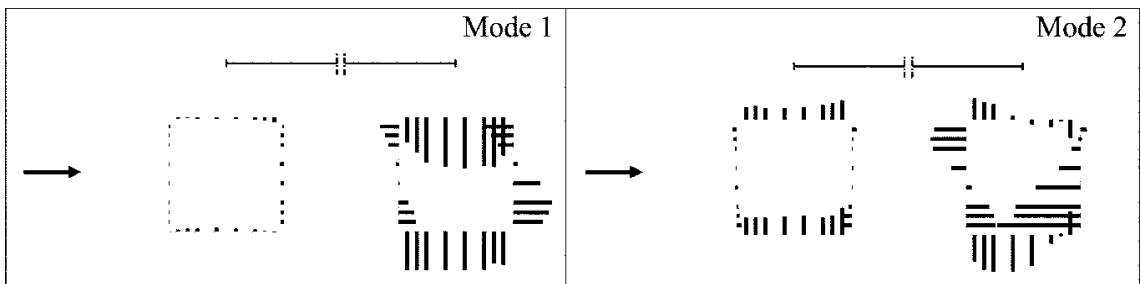


Fig. 12 First two mode shapes for the pair of cylinders in tandem arrangement for  $s/b=2$  in smooth flow

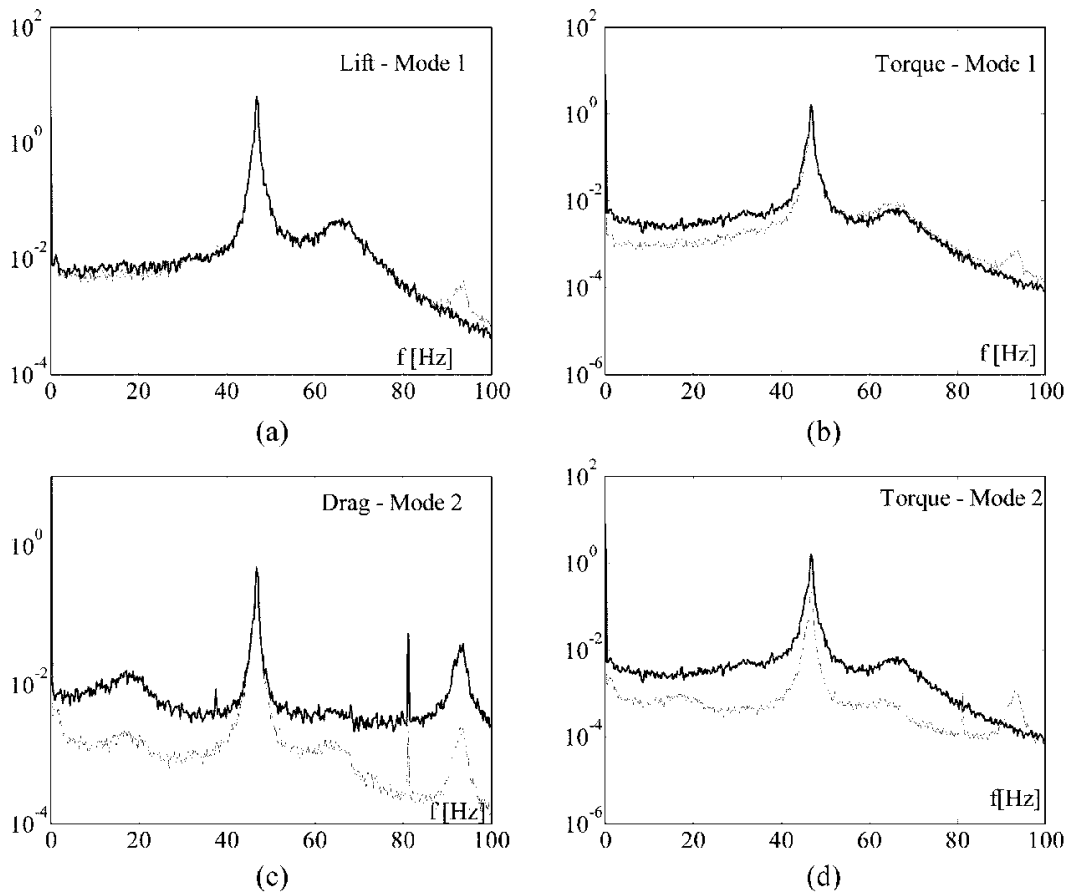


Fig. 13 Spectra of the partial (thick line) and total (thin line) aerodynamic coefficients for the pair of cylinder in tandem arrangement for  $s/b=2$  in smooth low

reproduces drag, and gives a contribution to torque at the Strouhal frequency. In addition, some coupling exists at twice the Strouhal frequency, where some drag-induced torque can be seen on the partial spectrum, which does not appear on the total spectrum.

In turbulent flow, however, this coupling between the different aerodynamic components does not exist. Mode one is a torque mode associated with out-of-phase lift forces on the two cylinders (Fig. 14), and therefore related to vortex shedding. Modes two to four are drag modes, associated with different pressure distributions on the windward and leeward faces of the upstream cylinder, and on the windward face of the downstream cylinder. The leeward face of the downstream cylinder never contributes to the fluctuating drag, which is the result of a narrow wake produced by flow reattachment. In particular, modes three and four seem to be related to the out-of-phase and in-phase effects of the oncoming turbulence on the two cylinders, while mode two is associated with the flow in the gap between the cylinders. Mode five and six are lift modes, deriving from in-phase lift forces on the two cylinders.

In Fig. 15 the first mode shape are shown, as evaluated separately on the upstream and

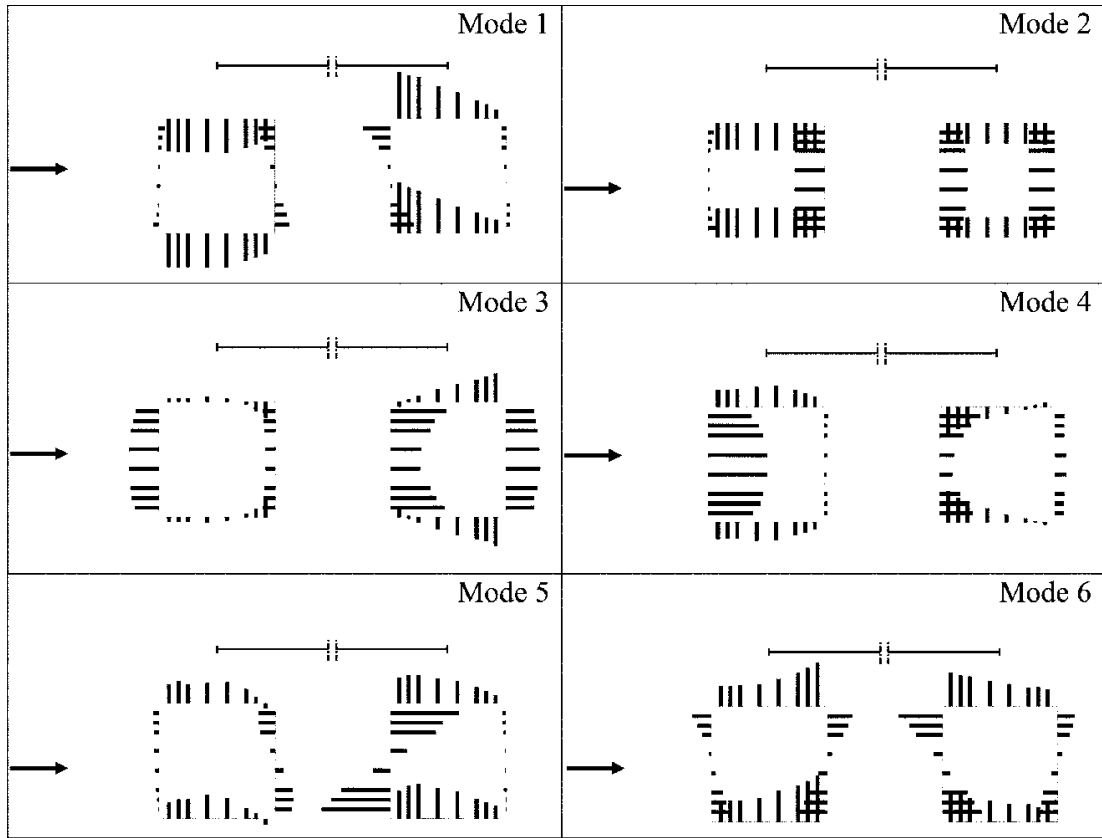


Fig. 14 First six mode shapes for the pair of cylinders in tandem arrangement for  $s/b=2$  in turbulent flow

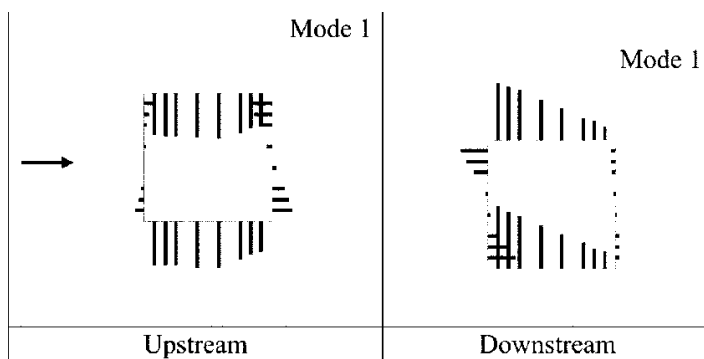


Fig. 15 First mode shape for the upstream and downstream cylinder in tandem arrangement for  $s/b=2$  in turbulent flow

downstream cylinders. Comparison with Fig. 14 shows that also in this case, if combined, modes one of the two cylinders exactly reproduce mode one of the pair.

### 5. Results for the pair of cylinders in side by side arrangement

Also for the side by side arrangement two different flow regimes were found (Ricciardelli and Vickery, 1998). In particular, in smooth flow and for very small separations ( $s/b \leq 2.5$ ), the two cylinders behave as a single, wide body, with a non-symmetric wake, being the symmetric mean flow pattern unstable. For larger separations in smooth flow, and for all the separations considered in turbulent flow ( $2 < s/b < 13$ ), the mean flow is symmetric, and the two cylinders behave as

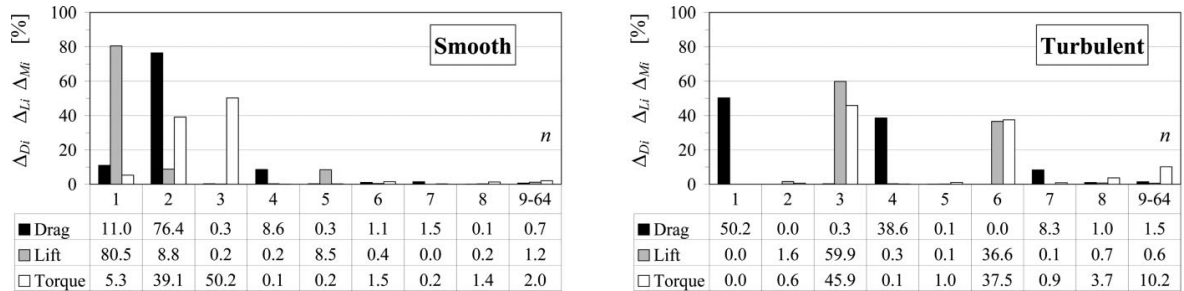


Fig. 16  $\Delta_{Dj}$ ,  $\Delta_{Lj}$  and  $\Delta_{Mj}$  coefficients for the pair of cylinders in side by side arrangement for  $s/b=2$  in smooth and in turbulent flow

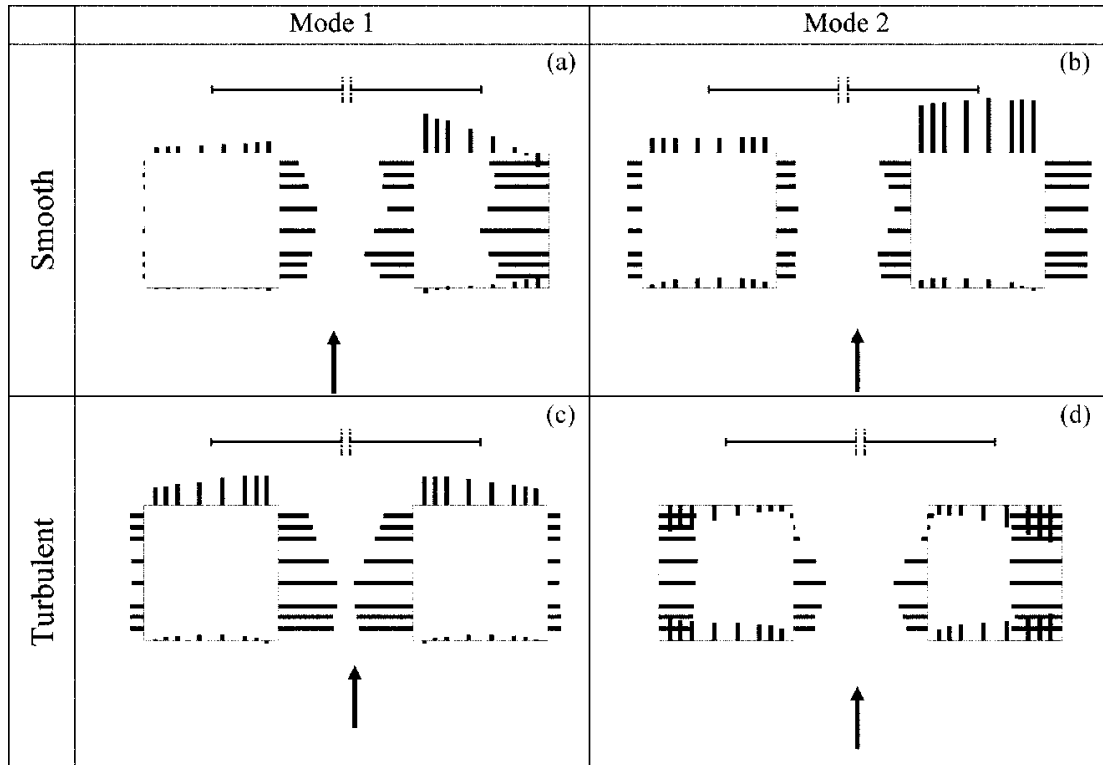


Fig. 17 First two mode shapes for the pair of cylinders in side by side arrangement for  $s/b=2$  in smooth and turbulent flow

separate bodies, whose interference depends on separation.

The complexity of the aerodynamic interaction at very small separations seems to make CPT unable to fully decouple the aerodynamic action on the pair of cylinders. In Fig. 16 the  $\Delta_{D_i}$ ,  $\Delta_{L_i}$  and  $\Delta_{M_i}$  coefficients are shown for the pair of cylinders at  $s/b=2$ , both in smooth and turbulent flow. While in turbulent flow mode one is a drag mode associated with wake turbulence (Fig. 17(c)), in smooth flow mode one (Fig. 17(a)) is mainly a lift mode associated with the non-symmetric gap flow (80.5% of the total lift), which causes some coupling with drag (11.0% of the total drag) and with torque (5.3% of the total torque). Again in smooth flow, mode two (Fig. 17(b)) is mainly a drag mode(76.4%), related to the wake pressures acting on one of the two cylinders, therefore a pronounced coupling with torque exists. Mode three in turbulent flow (Fig. 17(d)) is coupled lift-torque mode, where lift is due to the fluctuating pressures on the external faces of the pair, and torque is the result of out-of-phase wake pressures.

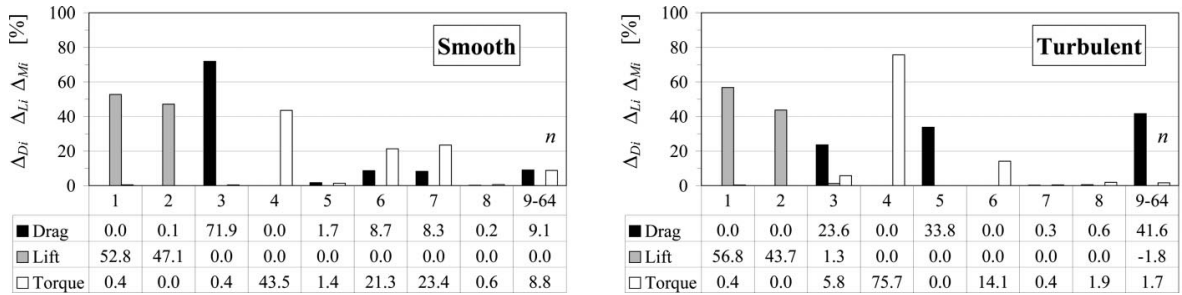


Fig. 18  $\Delta_{D_j}$ ,  $\Delta_{L_j}$  and  $\Delta_{M_j}$  coefficients for the pair of cylinders in side by side arrangement for  $s/b=13$  in smooth and turbulent flow

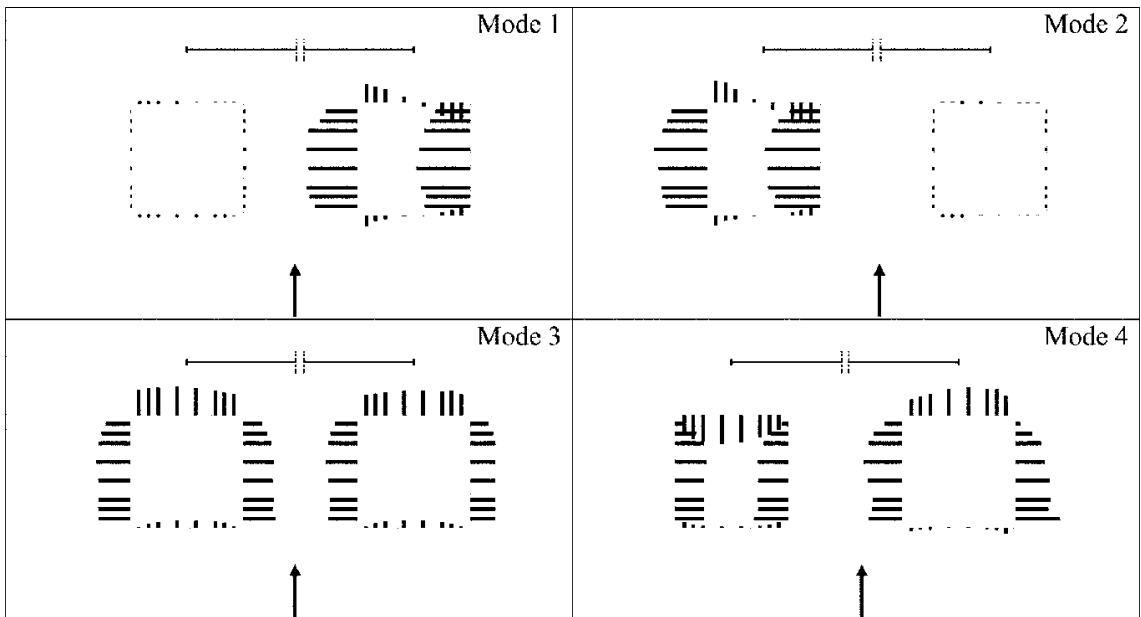


Fig. 19 First four mode shapes for the pair of cylinders in side by side arrangement for  $s/b=13$  in smooth flow

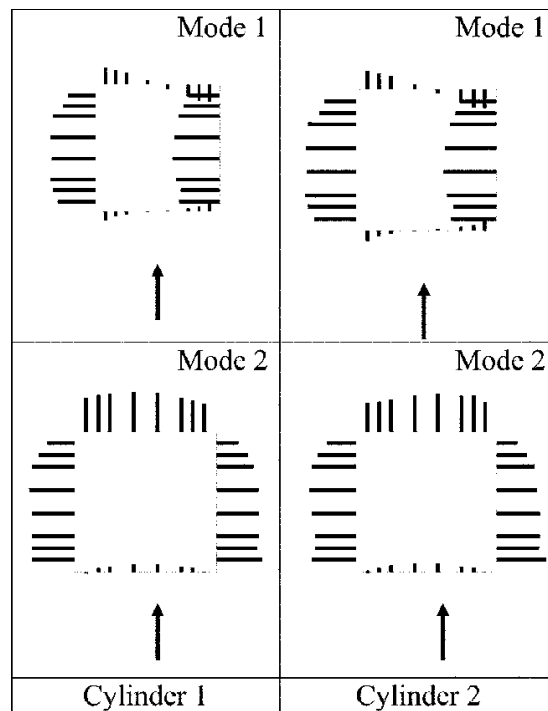


Fig. 20 First two mode shapes for the single cylinder in side by side arrangement for  $s/b=13$  in smooth flow

For very large separations, the aerodynamic interference tends to vanish, and the two cylinders behave independently. When CPT modes are evaluated for the pair, these can be either “local” modes, i.e., modes associated with pressure fluctuations on only one of the two cylinders, or “global” modes, to which pressure fluctuations of both cylinders correspond. In Fig. 18 the  $\Delta_{Di}$ ,  $\Delta_{Li}$  and  $\Delta_{Mi}$  coefficients are shown for the pair of cylinders at  $s/b=13$ , both in smooth and turbulent flow, indicating that a rather good degree of decoupling is achieved through CPT. For both flow regimes, modes one and two are lift modes, mode three is a drag mode and mode four is a torque mode. In Fig. 19 the first four mode shapes for the pair of cylinders are shown, for the smooth flow condition. Modes one and two are “local” lift modes, mode three is a symmetric, “global” drag mode, associated with in-phase wake pressure fluctuations on the two cylinders, and mode four is a torque mode associated with out-of-phase wake pressure fluctuations on the two cylinders.

It is interesting to note that when there is no aerodynamic interaction, the modes of the pair tend to be combinations of the modes of the cylinder taken separately. In this particular case, the first four modes of the pair are combinations of the first two modes of each of the two cylinders taken separately. To show this, in Fig. 20 modes one and two are shown, as evaluated separately on the two cylinders. It can be observed that modes one and two of cylinder one are coincident with the corresponding modes of cylinder two, and that mode one coincides with mode one of the single cylinder (Fig. 4), and mode two is similar to mode two of the single cylinder. This confirms that the two cylinders behave independently. In addition, comparison of Figs. 19 and 20 shows that the first four mode of the pair can be obtained as the following combinations of the modes of the single cylinder: (0, mode 1), (mode 1, 0), (mode 2, mode 2) and (mode 2, -mode 2).

## 6. Conclusions

In the present paper an application of CPT analysis to the pressure fluctuations on a square cylinder, and on a pair of square cylinders was presented. For the pair of cylinders, tandem and side by side arrangements were considered, with three values of the separation, and both smooth and turbulent flow conditions.

The results obtained confirm that a limited number of CPT modes allows to reproduce most of the aerodynamic excitation. In addition, it was shown that in most cases one single aerodynamic component corresponds to each mode. When many modes are associated with the same component, they are usually related to different physical causes of aerodynamic excitation. It was also found that the mode shapes of the pair of cylinders are in many cases combinations of the mode shapes found for the two cylinders evaluated separately. This confirms that the mode shapes are an intrinsic property of the system aerodynamics, rather than the mere product of a mathematical procedure.

The results shown here tend to corroborate the authors' belief that when CPT is applied a mathematical decoupling of the aerodynamic action is associated with a decoupling of the system physics, i.e., statistically independent modal processes correspond to physically independent phenomena, where these exist. Orthogonality of the mode shapes, however, is a further constraint introduced by POD, whose effects on the results of the decomposition is yet not fully understood. Although further study is required to fully understand the relationship between mathematical and physical decoupling, CPT appears to be a powerful tool to improve the understanding of the complex mechanisms of the aerodynamic excitation of bluff bodies.

## References

- Baker, C. (2000), "Aspect of the use of proper orthogonal decomposition of surface pressure fields", *Wind Struct., An Int. J.*, **3**(2), 97-115.
- Baker, C. (2001), "Unsteady wind loading on a wall", *Wind Struct., An Int. J.*, **4**(5), 413-440.
- Holmes, J.D., Sankaran, R., Kwok, K.C.S. and Syme, M.J. (1997), "Eigenvector modes of fluctuating pressures on low-rise building models", *J. Wind Eng. Ind. Aerodyn.*, **69-71**, 697-707.
- Kikuchi, H., Tamura, Y., Ueda, H. and Hibi, K. (1997), "Dynamic wind pressures on a tall building model - proper orthogonal decomposition", *J. Wind Eng. Ind. Aerodyn.*, **69-71**, 631-646.
- Lee, B.E. (1975), "The effect of turbulence on the surface pressure field of a square prism", *J. Fluid Mech.*, **69**, 263-282.
- Ricciardelli, F. (1994), "Aerodynamics of a pair of square cylinders", MSc Thesis, The University of Western Ontario, London, Canada.
- Ricciardelli, F. and Vickery, B.J. (1994), "Wind loads on a pair of long prisms of square cross section", *Proc. 3rd Italian Nat. Conf. Wind Eng. IN-VENTO-1994*, Rome, Italy.
- Ricciardelli, F. and Vickery, B.J. (1998), "The aerodynamic characteristics of twin column, high rise bridge towers", *Wind Struct. An Int. J.*, **1**(3), 225-241.
- Ricciardelli, F., de Grenet, E.T. and Solari, G. (2002), "Analysis of the wind loading of a bridge deck box section using Proper Orthogonal decomposition", *Proc. 3rd East European Conf. Wind Eng.*, Kiev, Ukraine.
- Solari, G. and Carassale, L. (2000), "Modal transformation tools in structural dynamics and wind engineering", *Wind Struct., An Int. J.*, **3**(4), 221-241.
- Tamura, Y., Ueda, H., Kikuchi, H., Hibi, K., Suganuma, S. and Bienkiewicz, B. (1997), "Proper orthogonal decomposition study of approach wind-building pressure correlation", *J. Wind Eng. Ind. Aerodyn.*, **72**, 421-431.
- Tamura, Y., Suganuma, S., Kikuchi, H. and Hibi, K. (1999), "Proper orthogonal decomposition of random wind pressure field", *J. Fluid and Struct.*, **13**, 1069-1095.